Available online at www.pelagiaresearchlibrary.com

Pelagia Research Library

Der Chemica Sinica, 2015, 6(5):137-146

Pelagia Research Library
ISSN: 0976-8505
CODEN (USA) CSHIA5

Synthesis of magnetic nanoparticles coated with palmitic acid and folic acid and study their interaction with prolactin

Hussain Kadhem Al-Hakeim[1], Mea'ad Mohammed Redha[1] and Ashour Hamood Dawood[2]

[1]*Department of Chemistry, Faculty of Science, Kufa University, Iraq*
[2]*The College of Pharmacy, Al-Mustansiriya University, Iraq*

ABSTRACT

In the present work, two coated magnetic nanoparticles (MNPs) were prepared using co-precipitation method of Fe_3O_4 followed by reaction of these MNPs with either folic acid or palmitic acid under optimum condition to produce coated MNPs called MNP@Folic and MNP@Palmitic, respectively. The synthesized coated MNPs were characterized and visualized by different advanced techniques. The interaction between the prepared MNPs and prolactin hormone was studied as a potential method for the extraction of PRL from biological fluids such as blood or for the immobilization of PRL on the surfaces of MNPs as a new application of these insoluble particles. MNPs have the ability to extract suitable amounts of PRL from solution. The differences between the quantities adsorbed from MNPS to another were little. Adsorption isotherms have S-shape on Giles classification for the adsorption isotherms. Freundlich's equation was applied for all the interaction processes indicating the heterogeneity of the forces on the surfaces that the PRL bound to. Desorption experiments showed very low desorption quantities indicating the magnitude of the forces that immobilize the PRL molecules on the surfaces of the prepared MNPs.

Keywords: Magnetic nanoparticles; surface modification; protein adsorption

---

INTRODUCTION

Magnetic (MNPs) are a class of NP which can be manipulated using magnetic field. Iron oxide MNPs with suitable surface chemistry show many interesting properties that can be employed in a variety of biomedical applications, such as magnetic resonance imaging[1], hyperthermia[2], drug delivery[3], and gene delivery[4]. These applications require MNPs such as iron oxide Fe_3O_4or modified MNPs with high magnetization values and very low particle size. For biological applications, surface coating of NPs should be polar to achieve high aqueous solubility and prevent aggregation. NPs can bind to biological molecules for transport to specific sites within the body [5].

Such particles commonly consist of magnetic core alone such as Fe_3O_4 or surface modified MNPs. Co-precipitation is a facile and convenient way to synthesize the magnetic core from aqueous Fe^{2+}/Fe^{3+} salt solutions by the addition of a base under inert atmosphere. The size, shape, and composition of the magnetic NPs very much depends on the Fe^{2+}/Fe^{3+} ratio, the reaction temperature, the pH value and ionic strength of the media[6, 7].

The interaction between proteins and NPs surface leads to the formation of proteins “corona” around NPs that largely defines their biological identity as well their potential toxicity[8, 9]. The ligands (groups) on the most of the common NPs are used for interaction with biological system [10].When NPs enter a biological fluid, proteins and other biomolecules compete for the nanoparticle surface, thus leading to the formation of a protein corona that defines the biological identity of the particle[11]. The binding of proteins on active surfaces induces conformational changes at secondary and tertiary structure levels [12, 13]. Therefore, determining the possible interaction between MNPs and different proteins is important. In the present research, two coated magnetic NPs were prepared by direct

surface modification of the original magnetic NPs and use these NPs to immobilize prolactin hormone on their surfaces for future medical applications.

MATERIALS AND METHODS

1-Synthesis of the coated Magnetic nanoparticles:
Iron Oxide nanoparticles(Fe_3O_4)
Fe_3O_4 MNPs were prepared by a modified co-precipitation described in [14]. Briefly, 0.04 mol of $FeCl_3 \cdot 6H_2O$ and 0.02 mol of $FeSO_4 \cdot 7H_2O$ were dissolved in 50 ml of 0.5 M HCl solution. Then, 500 ml of 1.5 M NaOH was added drop wise to the solution under vigorous stirring at 80 °C. The Fe_3O_4 precipitate obtained was separated using a magnet and was repeatedly washed with deionized water until the supernatant becomes neutral. The precipitate was dried at 50 °C for 4 h and then overnight at room temperature. For MNP@Folic acid synthesis, the same preparation method before obtaining Fe_3O_4 precipitate was followed. A volume of the obtained suspension was added to an oversaturated solution of folic acid at a ratio of 2:1 at 80 °C for 1 h under continuous stirring. After which, the precipitate was separated, washed, and dried. For MNP@Palmitic acid synthesis, the same preparation before obtaining Fe_3O_4 precipitate was again conducted. A volume of the obtained solution was added to an oversaturated solution of palmitic acid at a ratio of 2:1 at 80 °C for 1 h under continuous stirring. The suspension was then transferred into a watch glass and placed in an oven at 40 °C overnight until completely dried. Transmission electron microscopy (TEM) was used to visualize the morphology and size of the prepared MNPs.

2-Estimation of PRL Concentration by ELISA
Estimation of PRL concentration in solutions was measured using ELISA kits supplied by Monobind® Co. USA.

3-Estimation of Equilibrium Time of Adsorption
The time required for full saturation (equilibrium time) of the surface of MNPs (adsorbent) by PRL protein (adsorbate) has been determined by the following procedure:

100 µl of an initially fixed concentration (100ng/ml) of PRL solution was shaken with 50mg of each MNPs in an Eppindroff® tubes. Five tubes for each compound were prepared. The tubes were incubated with shaking. The PRL concentration in the solution was measured in the tubes every 30 minutes using ELISA technique. Before measurement, the tubes were centrifuged at 3000rpm for 5 minutes to precipitate the MNPs and the PRL level was estimated in the aspirated supernatant. The concentrations were plotted against time until the concentration of PRL in solution is constant (No further uptake of adsorbate by adsorbent as the time proceeds).

4-Adsorption Isotherms
One hundred microliters of PRL solution at concentrations0, 5, 10, 25, 50 and 100ng/ml were added to 50mg of each MNPs in an Eppindroff® tubes. The tubes were incubated with shaking for one hour which is the more than the equilibrium time obtained from the above paragraph. The PRL concentration in the solution was measured by using ELISA technique. Before measurement, the tubes were centrifuged at 3000rpm for 5 minutes to precipitate the MNPs and the PRL level was estimated in the aspirated supernatant. The amount of PRL adsorbed was calculated from the initial and final concentrations and the volume of solution.

$Q_e = x/m = V(C_o - C_e)/m$

x: The quantity adsorbed (ng)
V: Volume of solution (ml)
C_o: Initial concentration (ng/ml)
C_e: Equilibrium concentration (ng/ml)
m: Weight of adsorbent (MNPs)
Q_e values were plotted versus the equilibrium concentrations (C_e), the resulting diagrams are the adsorption isotherms that required for understanding and interpreting the systems under investigation.

5-Thermodynamics of the Adsorption of PRL on MNPs
The following concentrations of PRL in phosphate buffer (0, 5, 10, 25, 50 and 100ng/ml) were added to 50mg of every MNPs in an Eppindroff® tubes. The mixture was stirred for 30 minutes at different temperature (25, 35 and 45˚C). The mixture then centrifuge (6000rpm) and the supernatant then separated use ELISA techniques at 450nm to check the concentration value of PRL.The isotherms were constructed between PRL concentration in solution at equilibrium (C_e) and the amount of PRL that adsorbed on the NPs (Q_e). The isotherms were studied to find out the best equation applied for the practical results. The thermodynamic parameters (ΔH^o, ΔS^o and ΔG^o) parameters were calculated firstly using Van't Hoff's equation [15]

LnK_e=-ΔH°/RT + constant

Where ΔH°: enthalpy in reaction, K_e: maximum amount adsorbed, R: gas constant=8.314J/mol.˚K. By plotting LnK_e against 1/T and a straight line should be formed with a slope = -ΔH°/R.

In order to calculate the free energy change (ΔG°) of the adsorption process at a certain temperature, equilibrium constant of the adsorption –desorption process of urease on ceria nanoparticle should be calculated.

$K_e=Q_e*M/C_e*V_{(ml)}$

Where Keq: Equilibrium constant, Q_e: adsorption amount (µg/mg), M: mass of NP.(mg), C_e: Concentration of hCG at equilibrium µg/ml, and $V_{(ml)}$:volume of solution (ml). Then, free energy change can be calculated from the following equation:

$\Delta G^o = -RT \ln K_e$

Entropy (ΔS°) then calculated from the following formula [15, 16)

$\Delta S^o = (\Delta G^o - \Delta H^o)/T$

6-Desorption process:
To study the strength of the PRL-MNP interaction, the desorption experiments were carried out. In each case, PRL was adsorbed from solution onto the MNP compounds using a protocol similar to that for the adsorption using one initial PRL concentration (100µl) for each MNP compound. After incubation and centrifugation, as above described, the supernatant was removed and replaced by 100µl of normal saline solution (0.9%NaCl) to prevent PRL denaturation. The samples were further incubated at the room temperature to allow desorption to occur. Before measurement, the tubes were centrifuged at 3000rpm for 5 minutes to precipitate the MNP compounds and the PRL level was estimated in the aspirated supernatant. The desorption percentages were calculated from the ratio between the PRL quantity released into the solution on the PRL quantity desorbed initially on the MNP compound i.e., weight of PRL in 100µl/weight of PRL in 50mg:

%Desorbed=[(Ce/10)/(Qe/20)] *100%.

RESULTS

1-Charachterization of the prepared MNPs:
The size and morphology of the synthesized MNPs were confirmed via TEM. As shown in Figure 1, the shape of MNPs vary from spherical to cubic or truncated cubic (octahedral) structures for large particles with broad size distribution (20–100 nm). The TEM images showed that the Fe_3O_4@folic acid and Fe_3O_4@palmitic acid are larger than the MNPs.

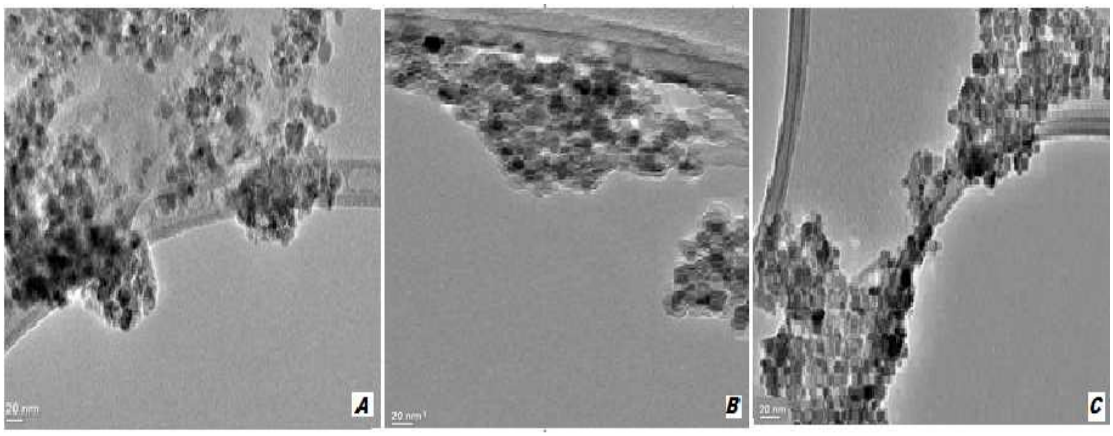

Figure (1): TEM images of the prepared NPs; (A)=Fe_3O_4, (B)=Fe_3O_4@Folic and (C)= Fe_3O_4@Palmitic

The FTIR spectrum of Fe3O4 NPs showed an important peak at approximately 450cm^{-1} due to the Fe-O bond in octahedral position while the peak of Fe–O stretch at 576cm^{-1} is in tetrahedral position.

The IR spectrum of Fe_3O_4@folic acid appears the bands at 3618 cm^{-1}, 3414 cm^{-1}, 3354 cm^{-1} due to the stretching of ν(OH), ν (NH_2), and ν(NH) groups respectively. The stretching of carboxylic groups appears the bands at 1705, 1691 cm^{-1} while the carbonyl of ketone shows at 1614, 1600 cm^{-1} the band in two positions refers to the groups found in different environments.

The IR spectrum of Fe_3O_4@palmitic acid displays the characteristic bands at 1415 and 1550cm-1 due to the symmetric and asymmetric carboxylate ion. The values at 2920 cm^{-1} and 2858 cm^{-1} correspond to asymmetric and symmetric stretching of the CH2-group. The band at 1614 cm^{-1} can be attributed to carbonyl group.

Figure 2 showed the weight loss percentage per degree of the synthesized MNPs. Maximum weight loss percentages occur around 100°C for Fe3O4 NPs, 68°C and 100°Cfor Fe3O4@Folic, and around 68°C and 100°C for Fe3O4@Palmitic.

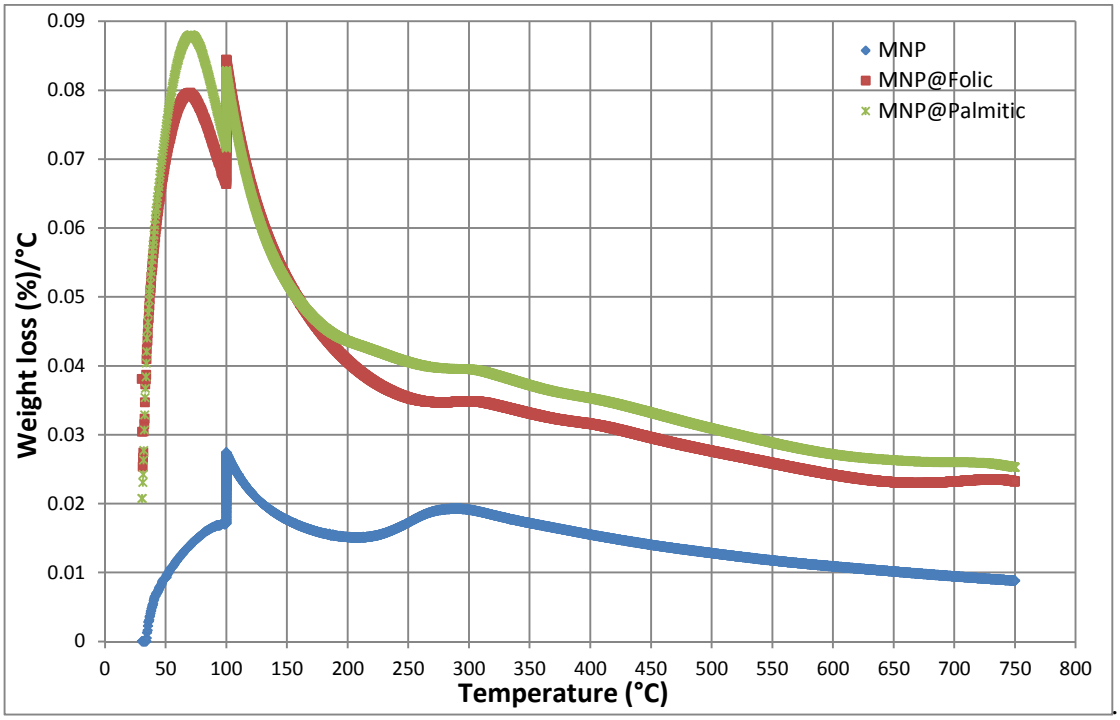

Figure (2): Weight loss percentage per degree of MNP as a function of increasing temperature

2-Properties of NPs after interaction with PRL hormone

After adsorption of PRL on the MNPs, MNP@Folic, and MNP@Palmitic, the formed composites were separated and visualized by TEM. Figures (3) are TEM images of the composites of PRL with MNPs, MNP@Folic, and MNP@Palmitic, respectively.

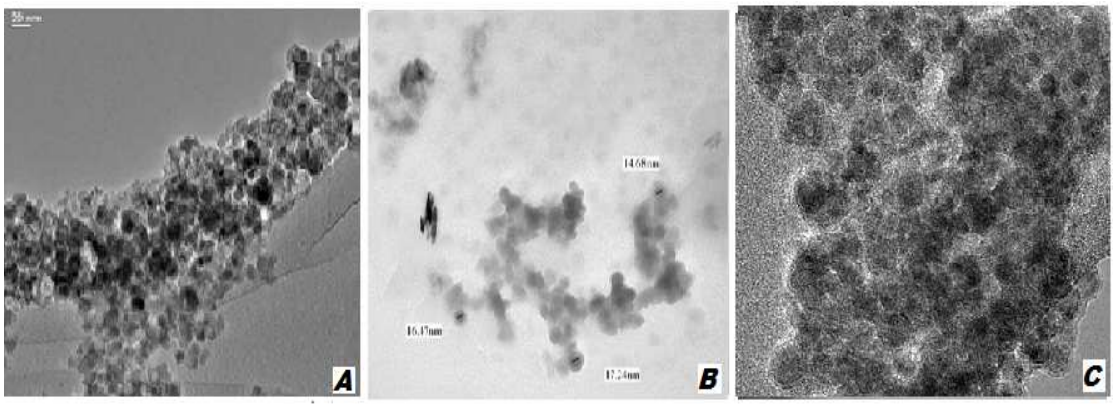

Figure 3: (A)**PRL-MNP composite, (B) PRL-MNP@Folic composite and (C) PRL-MNP@Palmitic composite**

3-Adsorption Process:

In order to obtain a better description for the behavior of the PRL adsorption on the surfaces of the NPs, the adsorption isotherm were constructed for the adsorption of PRL on MNPs, MNP@Folic, & MNP@Palmitic at 25°C (Figure 4).

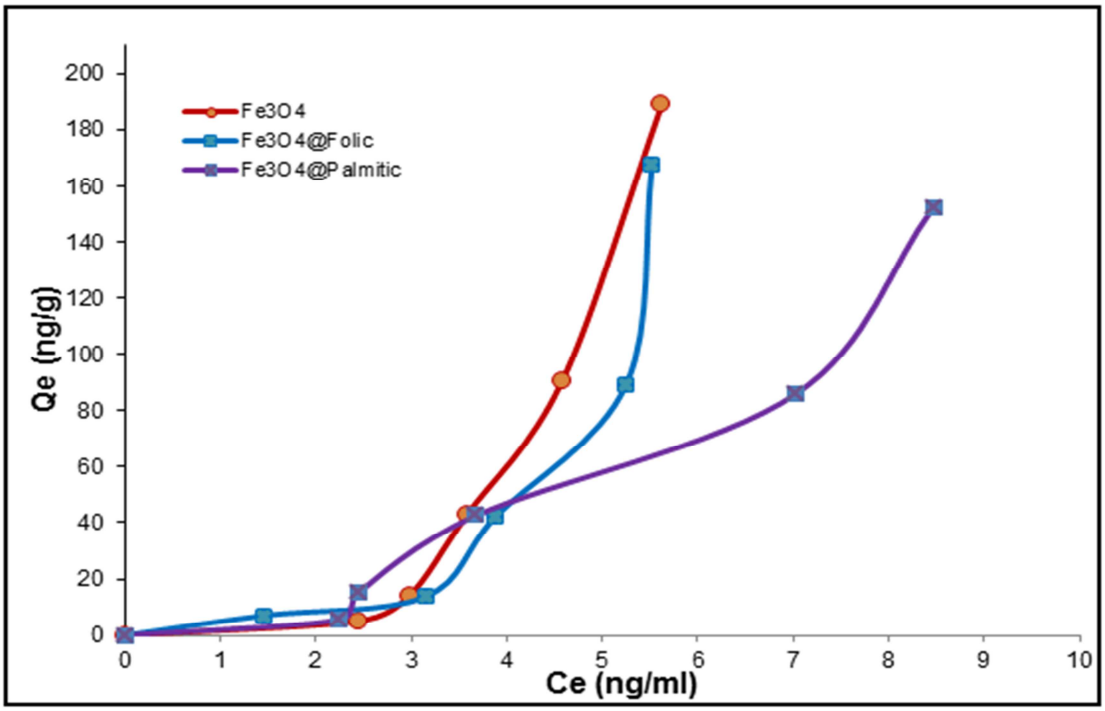

Figure (4): Adsorption isotherms of PRL hormone on the surface of MNP compounds 25°C

4-Applicability of Freundlich Adsorption Isotherms in the MNP-PRL systems

To clarify the surface forces homogeneity and interaction behavior of the MNP surfaces with PRL, adsorption isotherms of PRL on MNPs, MNP@folic, and MNP@palmitic were constructed in linear forms. The Freundlich model for the adsorption process were quite applied (Figures 5).

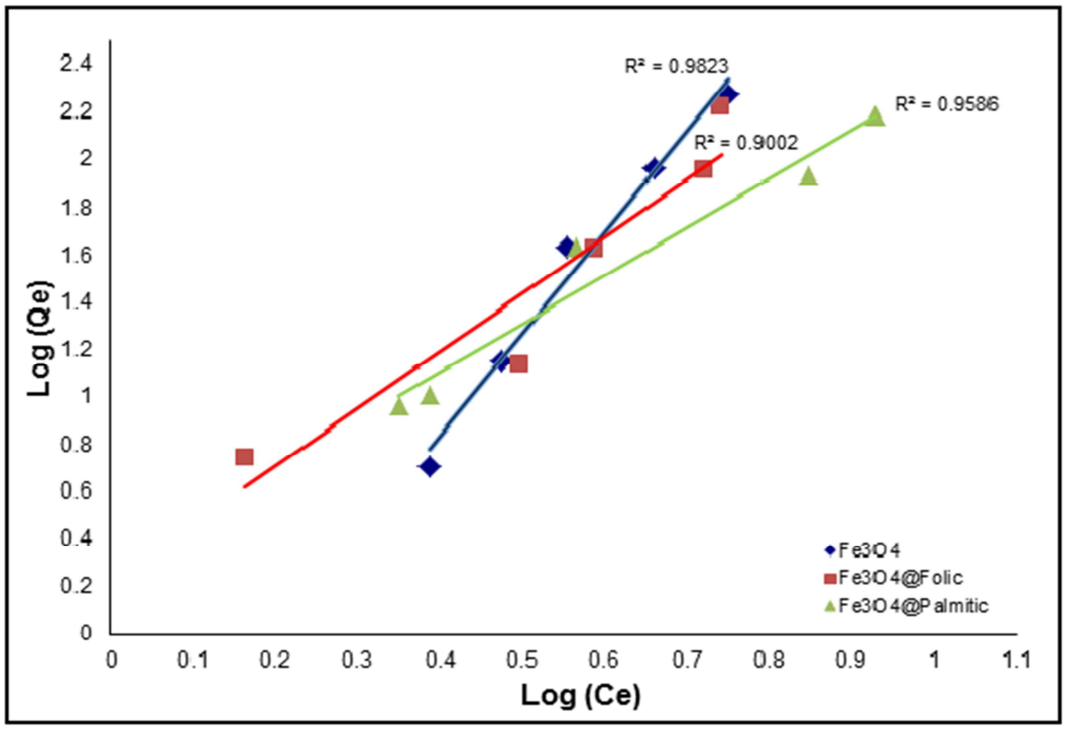

Figure (5): Linear form of the Freundlich equation for the adsorption of PRL on the surface of MNP compounds 25°C

5. Thermodynamics of the adsorption process:

Van't Hoff's plot for the adsorption of PRL on different MNPs are presented in Figure(16). The results of the thermodynamic parameters are presented in Table (2). The results showed that the adsorption processes is spontaneous, exothermic and produce a decrease in the entropy.

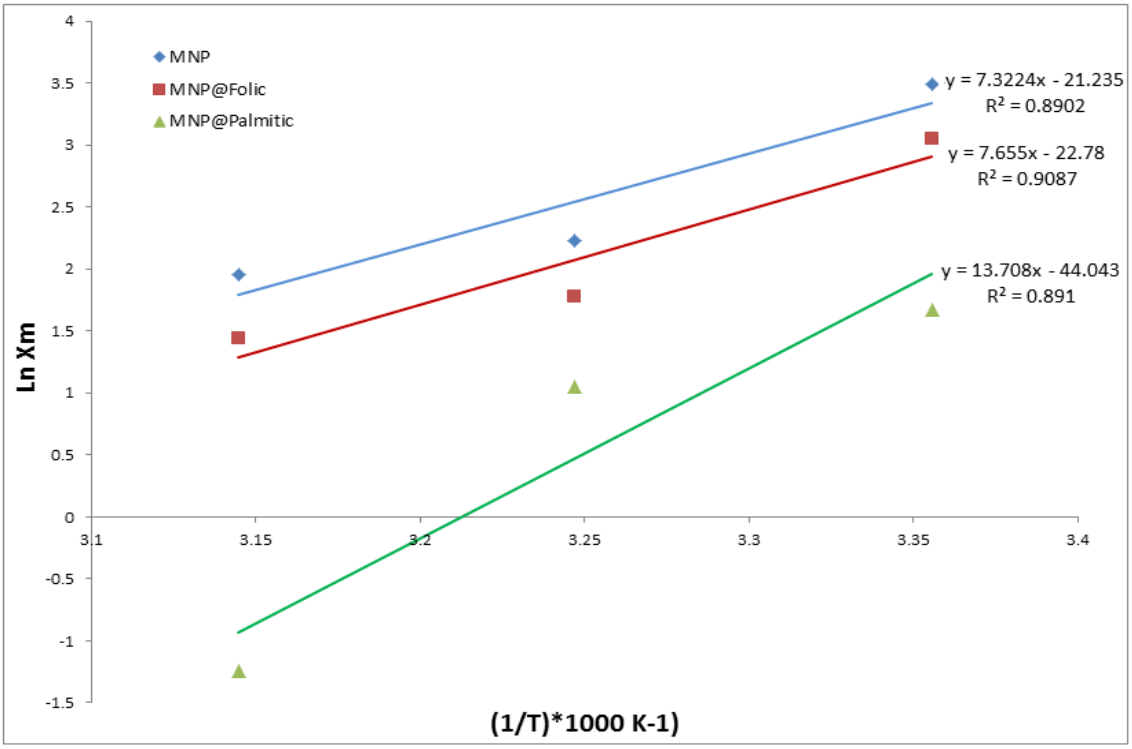

Figure (6): Van'tHoff's plot of the adsorption of PRL on MNP, MNP@Folic, and MNP@Palmitic acid at 25°C, 35°C, and 45°C

Thermodynamic parameters decreases in MNPs@Folic and MNPs@Palmitic in comparing with the original MNPs coated with an organic layers.

Table 1: Thermodynamic parameters of the adsorption of PRL on MNPs, MNP@Folic, and MNP@Palmitic

Nanoparticle	ΔG° kJ.mol^{-1}	ΔH° kJ.mol^{-1}	ΔS° J K^{-1}mol^{-1}
MNPs	**-8.64**	**-37.61**	**-97.21**
MNP@Folic	**-7.56**	**-32.28**	**-82.97**
MNP@Palmitic	**-4.15**	**-16.75**	**-42.29**

6-Desorption Process:

The results of the desorption process are presented in Figure (7) and showed that the desorption of PRL from NPs surfaces is dependent on temperature and the type of NPs. In MNPs and MNP@Folic, the desorption increases as temperature decreases while in MNP@Palmitic the case is inversed and the desorption increases as temperature increases.

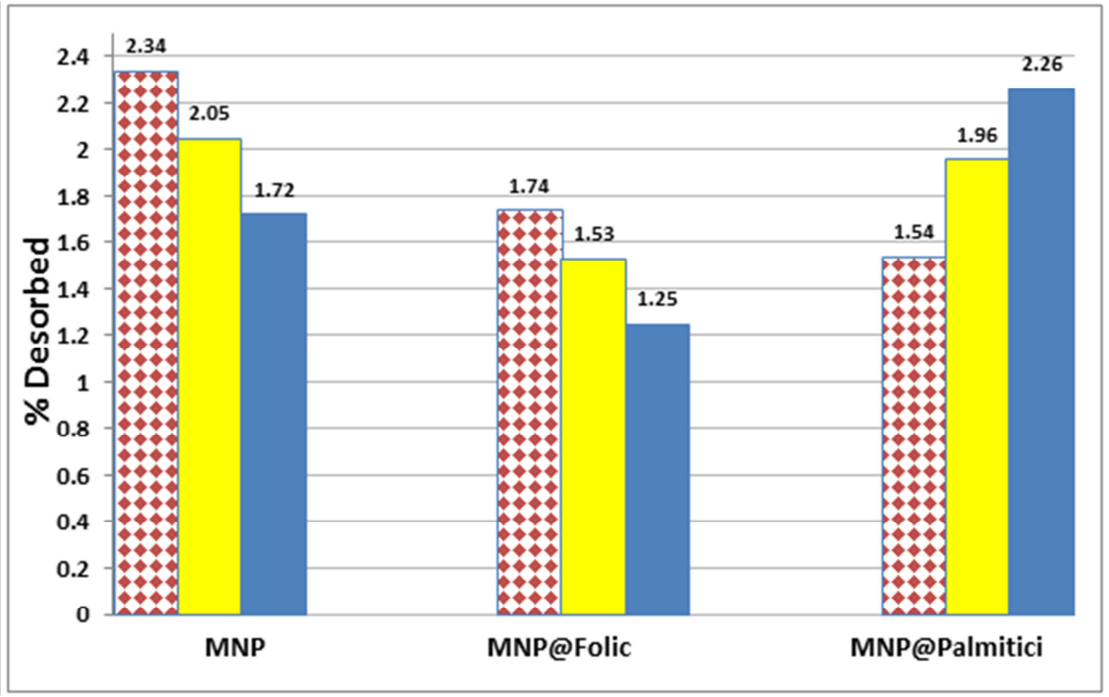

Figure (7) Desorption percentages of PRL from the surface of MNP, MNP@Folic, and MNP@Palmitic acid at 25°C (Diamond filled bar), 35°C (Light middle bar), and 45°C (Dark bar)

DISCUSSION

1-Charachterization of the prepared MNPs:
The increase in the particles size of the MNPs after the interaction with folic acid or palmitic acid leads to change in shape [17], as seen in the transformation of ball-shaped MNPs to cubic MNP-folic acid and MNP-palmitic acid. Furthermore, the folic acid and palmitic acid layers appear lighter than the MNP cubic core, indicating the formation of coated MNPs. The shapes did not changed in spite of vigorous washing and shaking of these MNPs dispersions.

Two distinguished peaks in the FTIR spectrum of Fe_3O_4 NPs are present; at approximately 450cm^{-1}, and 576cm^{-1} due to the stretch of Fe-O bond in the octahedral and tetrahedral position, respectively. This results are seen in other papers [18]. Bateer *et al* (2013)[19] showed the Fe-O peak of tetrahedral position at 590cm^{-1}. While Silva *et al* (2013)[17]found the band lies at 571cm^{-1}.This confirms the presence of the magnetic core in the NPs. The absorption peak at about 3252-3400cm^{-1} is observed that may be originated by hydroxyls (OH) present in water that adsorbed from the environment.

After the reaction between folic acid and Fe_3O_4, the carbonyl group shows shifting to a higher frequencies indicating the change took place in the molecules. Fe_3O_4 appears the different shifting in the FTIR spectrum from the free folic acid and MNP@Folic express the coordination occurs between the folic acid and the Fe ion. This conclusion can be confirmed through the disappearing of the hydroxyl groups band due to the partial or total ionization after binding with the active sites on the Fe_3O_4 NPs.
MNP@Palmitic acid spectrum showed bands that due to symmetric and asymmetric carboxylate ion indicating the formation of new bond between the carboxylate radical and the outer –OH groups on the MNPs. There is a peak of the weight loss from Fe3O4 around 68.3°C due to the loss of the adsorbed water. In general, all the prepared MNPs showed a highest weight loss percentages at 100°C as a result of loss of water that is bound weakly from the structure of the MNPs. Gradual increase in weight loss percentage also occurs as temperature increases owing to loss of water that tightly bound to the structure of the MNP. There is also another peak of weight loss occurred at approximately 300 °C, which are attributed to the loss of organic compartment from the structure of the Fe_3O_4@Folic and Fe_3O_4@Palmitic. These two sharp peaks appeared at 100 and 300 °C indicating the formation of new structure between the organic (folic acid or palmitic acid) and inorganic (Fe_3O_4) parts.

From the above results, the following structural depictions are suggested. These schemes indicated electrostatic forces between the MNP and the acids.

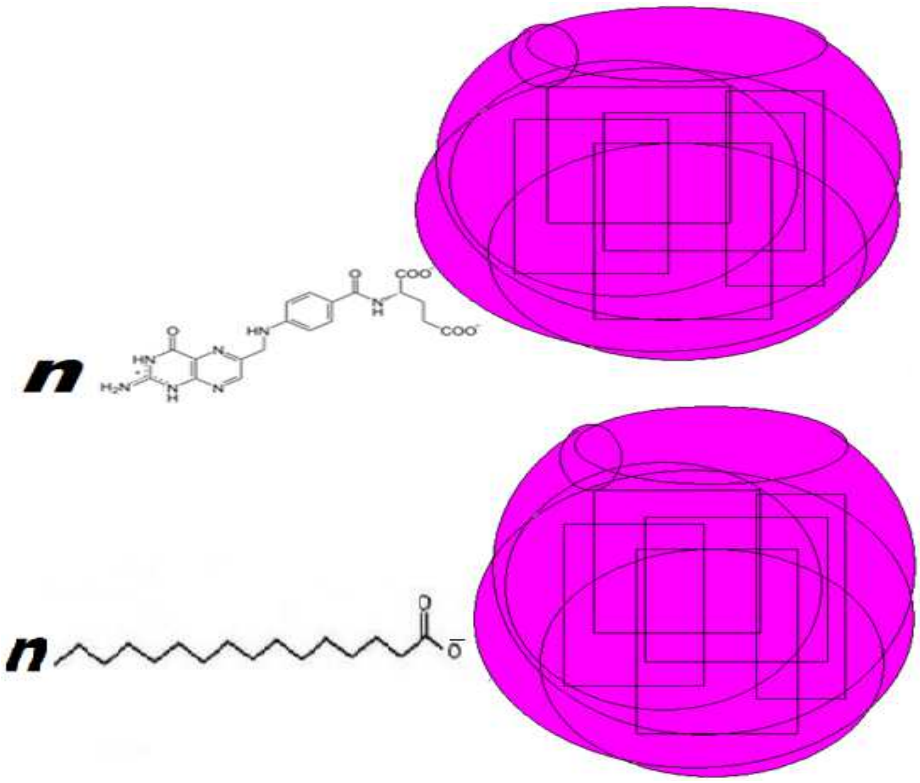

Figure 3: Suggested structural depictions of the prepared MNP@Folic (above) and MNP@Palmitic (Below)

2-Properties of NPs after interaction with PRL hormone

TEM images of the composites of PRL with MNPs, MNP@Folic, and MNP@Palmitic composites (Figure 3), showed round particles larger than the original (uncoated) particles due to the saturation of the particle surfaces with proteins. The interaction between proteins and NPs surface leads to the formation of proteins "corona" around NPs that largely defines their biological identity as well their potential toxicity and other vital properties[20, 21]. The following structural depiction for the MNP-PRL composite are suggested in the Figure .

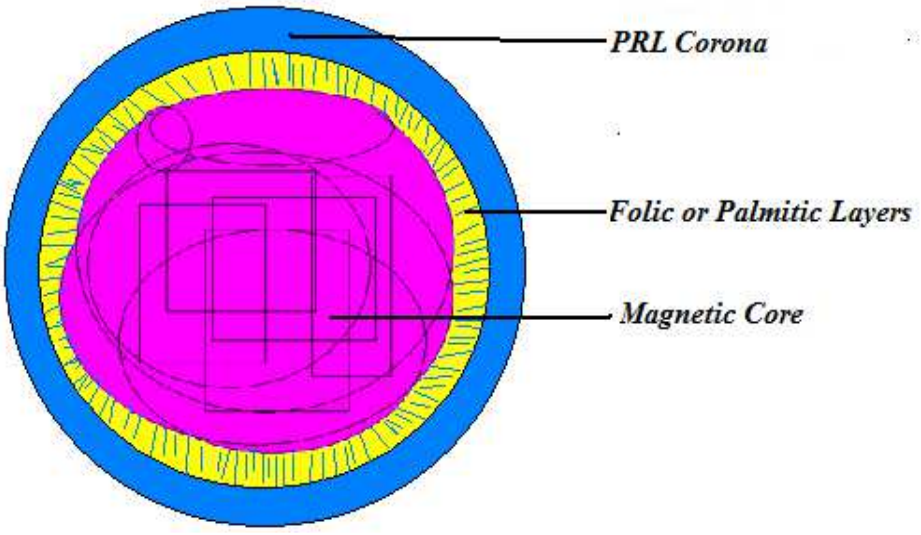

Figure 3: Suggested structural depictions of the nanoparticle-PRL composite

The nanoparticle surface is immediately occupied by proteins with high concentrations and high association rate constants and successively by proteins having lower concentrations but a higher affinity [20].Competitive absorption of proteins is influenced by several factors such as electrostatic interactions, protein stability, and kinetic parameters [22].

NPs have significant adsorption capacities due to their relatively large surface area, therefore they are able to bind or carry other molecules such as chemical compounds, drugs, and proteins attached to the surface by covalent bonds or by adsorption. Hence, the physicochemical properties of NPs, such as charge and hydrophobicity, can be altered by attaching specific chemical compounds, peptides or proteins to the surface [23, 24].

3-Adsorption process and isotherms.
The isotherms in Figure 4 showed a slight increase in the quantity of the adsorbed PRL (Q_e) as the PRL equilibrium concentration (Ce) increases. This means that the adsorption tendency is very low at the low PRL concentration and showed a rapid increase in Qe at higher PRL concentration. There is a slight difference between the quantities adsorbed of PRL on the nanoparticle surfaces.

The change in the PRL concentration showed a mild difference among MNPs, MNP@Folic, and MNP@Palmitic composites. These results indicated a mild dependence of the adsorption process on the organic part of the MNPs.While binding of proteins to planar surfaces often induces significant changes in secondary structure, the high curvature of NPs can help proteins to retain their original structure [25]. The size of NPs determines the surface curvature: this means that NPs of large size have low surface curvature, while those of small size possess high surface curvature, and curvature is lowest for a planar surface.

Most proteins have a tertiary structure that is spheroidal with a major and minor axis, rather than spherical. Hence, initial adsorption to a surface can occur in more than one orientation with respect to the surface. Two fundamentally different approaches can be used to conjugate proteins to NPs. The first approach uses direct covalent linkage of the protein to the particle surface. The second method uses non-covalent interactions between the particle and protein to generate supra molecular assemblies. Both of these approaches have strengths and limitations, and hence have a place in the bionanotechnology[10].

Figure 5 showed the Freundlich isotherm is obeyed for the adsorption of PRL on the surfaces of the synthesized MNPs. When the adsorption data obey the linear form of Freundlich equation, the adsorption process obeys the Freundlich isotherm which is used to interpret the adsorption data of the investigated systems. Freundlich isotherm implies different forces on the surface or on the PRL molecules to produce the heterogeneity. PRL adsorption on the surfaces of MNP@Palmitic acid obeys both equations. However, the strength of the surface–protein attraction and the intermolecular repulsions should be considered. In addition, repulsions depend very strongly on the shape and size of the molecules. Therefore, a proper treatment of the equilibrium adsorption isotherms requires a theoretical description that includes all of these components at the molecular level.

4. Thermodynamics of the adsorption process:
The results in Figure 6 showed that the adsorption processes is exothermic and produce a decrease in the entropy leading to more regularity and less random due to the fixation of PRL on the NPs surfaces. Thermodynamic parameters decreases as the original MNPs coated with an organic layers. This result is due to the saturation of the active sites on the MNPs with organic molecules leading to decrease the affinity for adsorption and subsequent decrease in the thermodynamic parameters that drive the adsorption process.

Thermodynamic parameters, extracted by different models [26], can define quantitative description for the adsorption of proteins and peptide on different surfaces that involve the conformational changes [27]. The study of the materials biocompatibility starts with the analysis of protein adsorption on surfaces [28].

Study of a variety of nanoparticle surfaces and proteins indicates that the perturbation of protein structure still happens to varying extents as seen in many researches. The unfolding kinetics of some proteins when adsorbed onto NPs shows that upon adsorption, the proteins show a conformational change at both secondary and tertiary structure levels [20, 29]. Many studies have found that loss of α-helical content occurs when proteins are adsorbed onto NPs, with or without an increase in β-sheet [25, 29]. These findings are supported by a recent study that showed that the adsorption of protein on solid surfaces is driven by conformational changes that leads to a negative entropy change [30, 31].

5-Desorption Process:
The results in Figure 7 showed that the desorption percentages were very low indicated a strong force3s between the surface and protein molecules that may be due to formation a type of chemical bonds between the NPs surface and PRL molecules. Solvation power increases with increasing temperature while the decrease in temperature may reduce any chemical attraction between PRL and MNPs. Keisel *et al*(2014) [31] introduced another factor, the mobility of the proteins at the interface, affecting the desorption.

CONCLUSION

In this study, two coated MNPs, namely, MNP@Folic acid and MNP@Palmitic acid, were prepared and characterized. These MNPs can efficiently adsorb and immobilize PRL, thereby exhibiting their potential use in medical applications. Desorption quantities of PRL from the surface of the MNPs were generally low and the adsorption processes were exothermic.

REFERENCES

[1] Urries I, Muñoz C, Gomez L, Marquina C, Sebastian V, Arruebo M, Santamaria J. *Nanoscale.***2014**;6(15):9230-40.
[2] Mohammad F, Yusof NA. *J Colloid Interface Sci.***2014**;434C:89-97.
[3] Unterweger H, Tietze R, Janko C, Zaloga J, Lyer S, Dürr S, Taccardi N, Goudouri OM, Hoppe A, Eberbeck D, Schubert DW, Boccaccini AR, Alexiou C. *Int J Nanomedicine.* **2014**;9:3659-76.
[4] Kami D, Kitani T, Kishida T, Mazda O, Toyoda M, Tomitaka A, Ota S, Ishii R, Takemura Y, Watanabe M, Umezawa A, Gojo S. *Nanomedicine.***2014**; 6:1165-74.
[5] Akerman ME, Chan WC, Laakkonen P, Bhatia SN, Ruoslahti E. *Proceedings of the Nat Acadf Sci USA.* **2002**; 99 (20): 12617–12621.
[6] Lu AH, Salabas EL, Schuth F. *Angew Chem Int Ed*. **2007**;46(8):1222–1244.
[7] Lynch I, Dawson KA, Linse S. *Sci STKE*. **2006**; 327: pe14.
[8] Jedlovszky-Hajdú A, Bombelli FB, Monopoli MP, Tombácz E, Dawson KA. *Langmuir.***2012**;28(42):14983-14991.
[9] Hayashi Y, Miclaus T, Scavenius C, Kwiatkowska K, Sobota A, Engelmann P, Scott-Fordsmand JJ, Enghild JJ, Sutherland DS. *Environ Sci Technol.***2013**;47(24):14367-14375.
[10] Cedervall T, Lynch I, Lindman S, Berggard T, Thulin E, *et al*. *Proc Natl Acad Sci USA*. **2007**; 16: 2050–2055.
[11] Docter D, Distler U, Storck W, Kuharev J, Wünsch D, Hahlbrock A, Knauer SK, Tenzer S, Stauber RH. *Nat Protoc.***2014**;9(9):2030-44.
[12] Wang J, Jensen UB, Jensen GV, Shipovskov S, Balakrishnan VS, Otzen D, Pedersen JS, Besenbacher F, Sutherland DS. *Nano Lett.***2011**;11(11):4985-4991.
[13] Cukalevski R, Lundqvist M, Oslakovic C, Dahlbäck B, Linse S, Cedervall T. *Langmuir.***2011**;27(23):14360-9.
[14] Zhang Z, Zhang Y. *J. Acta of Northwest Sci-Tech Univ Agric Forestry*, **1998**, 26(2): 94–98.
[15] Jackson M. Moleular and Cellular Biophysics. Cambridge University Press: New York, *Humana Press Inc., Totowa, NJ*. **2006**. pp:261-275.
[16] You Q, Antony J, Sharma A, Nutting J, Sikes D, Meyer D. *J Nanopart Res.***2006**; 8: 489–496.
[17] Silva VAJ, Andrade PL, Silva MPC, Bustamante AD, Valladares LDS, Aguiar JA. *J Magn and Magn Mat.***2013**; 343:138–143.
[18] Casillas PEGa, Gonzalez CAR, Pérez CAM.Infrared Spectroscopy of Functionalized Magnetic Nanoparticles. Mexico, ISBN: 978-953-51-0537-4, InTech. **2012**.pp:22-35.
[19] Bateer B, Qu Y, Meng X, Tian C, Du S, Wang R, Pan K, Fu H.. *J Magn and Magn Mat.***2013**; 332 :151–156.
[20] Wu XY,Narsimhan G. *Biochim Biophys Acta*. **2008**; 1784: 1694-1701.
[21] Rana S, Yeh YC, Rotello VM. *Curr Opin Chem Biol.***2010**; 14(6): 828–834.
[22] Aili, D., Enander, K., Rydberg, J., Nesterenko, I., Bjorefors, F., Baltzer, L., Liedberg B. *J. Am. Chem. Soc.***2008**,130: 5780-5788.
[23] De M, Rana S, Rotello VM. *Macromol Biosci* **2009**, 9: 174–178.
[24] Zhang Q, Zhao Q, Zhang Y, Han N, Hu L, Zhang C, Jiang T, Wang S. *J Colloid Interface Sci.***2014**, 434C:113-121.
[25] Li Fei and Sarah Perrett. *Int J Mol Sci.***2009**;10, 646-655
[26] Zhong ED[1], Shirts MR. *Langmuir.***2014**;30(17):4952-61.
[27] Chilamkurthi S, Sevillano DM, Albers LH, Sahoo MR, Verheijen PJ, van der Wielen LA, den Hollander JL, Ottens M.*J Chromatogr A.***2014**;1341:41-9.
[28] Vertegel A, Siegel R, Dordick J. *Langmuir*. 2004;20: 6800–6807.
[29] Wang J, Zheng S, Shao Y, Liu J, Xu Z, Zhu D. *J Colloid Interf Sci.***2010**; 349,293-299
[30] Silva GL, Marques FS, Thrash ME Jr, Dias-Cabral AC. *J Chromatogr A.***2014**;1352:46-54.
[31] Kiesel I, Paulus M, Nase J, Tiemeyer S, Sternemann C, Rüster K, Wirkert FJ, Mende K, Büning T, Tolan M. *Langmuir*.**2014**;30(8):2077-2083.